Available online at www.sciencedirect.com
ScienceDirect
Journal of Computational Physics 220 (2006) 409–421
JOURNAL OF COMPUTATIONAL PHYSICS
www.elsevier.com/locate/jcp

# A high order finite element discretization with local absorbing boundary conditions of the linear Schrödinger equation ☆

Isaías Alonso-Mallo [a,*], Nuria Reguera [b]

[a] *Departamento de Matemática Aplicada, Facultad de Ciencias, Universidad de Valladolid, C/Dr. Mergelina s/n, 47011 Valladolid, Spain*
[b] *Departamento de Matemáticas y Computación, Universidad de Burgos, Avda. Cantabria, s/n, Burgos, Spain*

Received 28 November 2005; received in revised form 4 April 2006; accepted 17 May 2006
Available online 7 July 2006

**Abstract**

The goal of this paper is to obtain a high order full discretization of the initial value problem for the linear Schrödinger equation in a finite computational domain. For this we use a high order finite element discretization in space together with an adaptive implementation of local absorbing boundary conditions specifically obtained for linear finite elements, and a high order symplectic time integrator. The numerical results show that it is possible to obtain simultaneously a very good absorption at the boundary and a very small error in the interior of the computational domain.


*AMS:* 65M12; 65M20; 65M99

*Keywords:* Linear Schrödinger equation; Finite element; Local absorbing boundary conditions

## 1. Introduction

We consider the initial value problem for the linear time dependent Schrödinger equation

$$\begin{aligned} &\partial_t u(x,t) = \frac{-\mathrm{i}}{c}(\partial_{xx} u(x,t) + V(x)u(x,t)), \quad x \geqslant 0, \ \ t \geqslant 0, \\ &u(0,t) = 0, \\ &u(x,0) = u_0(x), \end{aligned} \tag{1.1}$$

where $V(x)$ is the potential and $c$ is constant (in this paper we will suppose that $c < 0$, the case $c > 0$ is similar). There are several applications of (1.1), for example in quantum mechanics [16], optics [24] and seismic wave propagation [10].

☆ This work has obtained financial support from MCYT under project MTM 2004-08012 cofinanced by FEDER funds and JCYL VA103/04.
* Corresponding author. Tel.: +34 983423769; fax: +34 983423013.
*E-mail addresses:* isaias@mac.uva.es (I. Alonso-Mallo), nreguera@ubu.es (N. Reguera).

0021-9991/$ - see front matter 
doi:10.1016/j.jcp.2006.05.022

The study of the well-posedness of (1.1) in the original unbounded domain $\mathbb{R}^+ = [0, +\infty)$ is not complicated. Take the Hilbert space $X = L^2(0, +\infty)$ with the scalar product

$$\langle f, g \rangle = \int_0^\infty f(x)\overline{g(x)}\,\mathrm{d}x,$$

and we suppose that $V \in L^\infty(0,\infty)$ and we consider $D(A) = H^2(0,\infty) \cap H_0^1(0,\infty)$. Then, it suffices to take into account that the operator $A : D(A) \to X$ given by

$$(Au)(x) = \frac{-\mathrm{i}}{c}(\partial_{xx}u(x) + V(x)u(x))$$

for $u \in D(A)$ and $x \in (0,\infty)$ can be written as $A = \mathrm{i}A_0 + B$ where $A_0$ is a selfadjoint operator and $B$ is a bounded perturbation. Therefore $A$ is the infinitesimal generator of a $C_0$ semigroup (see [20]) and we deduce that (1.1) is well-posed in $X$.

However, for the numerical approximation of (1.1), we need to restrict the computation to a finite computational subdomain of $\mathbb{R}^+$. Therefore, we need to use artificial boundary conditions in order to obtain a practical numerical scheme. This problem is the subject of a wide number of papers in the literature. It is possible to find a large list of references in the reviews [17,18,26].

Although these artificial boundary conditions have been studied for all kinds of equations, they are mainly used for wave propagation problems, including wave equation, hyperbolic systems and Schrödinger equation, which are the cases focused in [18].

There are three main kinds of methods to obtain a good approximation to the exact solution in the computational domain. The absorbing layers are based in the use of artificial source terms designed to dissipate the solution arriving at the boundary. The main drawback is that it is necessary to enlarge artificially the computational domain. There is a resurgence of these techniques, referred to as perfectly matched layer, from the publication of the paper [9], where an absorbing layer without reflection to the interior domain is proposed (see also [10] for the case of the Schrödinger equation).

The transparent boundary conditions (TBCs) are obtained with the aim that the solution in the computational window equals to the exact solution. Usually, the trouble here is that these TBCs can be non-local. This is the case for (1.1), see for example [5–8,24,25].

Finally, absorbing boundary conditions (ABCs) are defined as an approximation of TBCs in a such a way that the reflection to the interior of the computational domain is small but with the advantage that these boundary conditions are now local [11,13,14].

As it is noted in the conclusions of [18], another usual advantage of the ABCs is that they are easier to use, mainly when the geometry of the artificial boundary can be fixed in a simple way. In [18], the author studies for the wave equation an adaptive implementation where the order of the ABCs varies automatically with an optimal of the interpolatory nodes. In [1,2] ABCs for the Schrödinger equation discretized in space with finite differences are studied. In these works we have found weak instabilities when the order of absorption increases. The origin of this phenomenon is that the matrices of the semidiscrete problems are non-normal. Therefore, the fact that the spectral abscissa is negative is a necessary but non-sufficient condition in order to obtain well-posedness. Therefore, it seems that the previous adaptive strategy could be non-suitable for the Schrödinger equation, as it is noticed in [18]. As an alternative, we have proved in [3] that it is possible to fix the order of absorption and to choose adaptively the interpolatory nodes in order to absorb in an optimal way the solution arriving to the boundary. The trick is to use the classical Prony's algorithm [19] to approximate the solution.

In this paper we are interested in showing that it is possible to take advantage of the simplicity of the problems which arise with these ABCs in order to obtain a very good approximation along with a very high absorption at the boundary.

The first trouble is that in the literature the ABCs for spatial discretizations of (1.1) are only obtained for low order finite difference discretizations which are not suitable to obtain an efficient spatial discretization. Therefore, we obtain in Section 2 TBCs for a discretization by means of linear finite elements. Similarly to the case of finite differences, these TBCs are non-local; then, also in Section 2, we construct local ABCs for linear finite elements and we derive an adaptive technique for its implementation which is similar to that used in [3] for second order finite differences. The numerical experiments show that the absorption is very good and similar to that observed in [3].

However, we show in Section 4 that the accuracy of the spatial discretization in the interior of the computational domain is also similar to the one in [3] and it cannot be considered satisfactory. Therefore, we show that it is possible to combine the use of these new ABCs implemented with linear finite elements near the boundary, with cubic finite elements in the interior of the computational domain. We remark that it is plain to generalize these techniques for the use of other high order finite element discretizations through the weak formulation of (1.1).

We also analyze the time discretization in Section 3. We remark that, for TBCs, the discretizations in the literature are usually of low order because of the difficulty of the implementation of a non-local boundary condition [5–8,24,25]. In our case, the implementation is straightforward and we consider a symplectic Runge–Kutta method, but other usual time integrators can be easily considered. Now, the incorporation of ABCs leaves to a problem which is not already Hamiltonian, therefore we discuss how to choose the time integrator depending of its stability region.

In this way, we achieve a very good absorption at the boundary and simultaneously a small error of the full discretization.

Finally, we note that these ideas can be extended to other cases. For example, we have studied in [4] the use of ABCs for finite differences discretizations of a nonlinear cubic Schrödinger equation with good results of absorption. We think that it is possible to extend the implementation in [4] to a high order numerical scheme, as it is shown here for the linear case. On the other hand, it is also possible to consider the 2D-case. For instance, ABCs for a rectangular boundary are obtained in [1], although a better option, in forthcoming works, could be to consider a circular boundary in order to avoid the difficulties at the corners.

## 2. Space discretization with finite elements

We denote $\mathscr{V} = H_0^1(0,+\infty)$ and, for $u, w \in \mathscr{V}$, we consider the sesquilinear form $a(u,w)$ given by

$$a(u,w) = -\frac{\mathrm{i}}{c}\left[-\int_0^{+\infty} \partial_x u(x)\partial_x\overline{w(x)}\,\mathrm{d}x + \int_0^{+\infty} V(x)u(x)\overline{w(x)}\,\mathrm{d}x\right].$$

Then we consider the weak formulation of (1.1):

$$\text{find } u(t) \in \mathscr{V} \text{ such that } u(0) = u_0 \text{ and } \left\langle \frac{\mathrm{d}u}{\mathrm{d}t}, w\right\rangle = a(u,w), \quad \text{for each } w \in \mathscr{V}. \tag{2.1}$$

We want to solve numerically this problem using the finite element method for its spatial discretization. However, the first inconvenient is that this problem is defined in an infinite spatial domain and in order to integrate it numerically it is necessary to work in a finite subdomain and to use artificial boundary conditions. For the space discretization of (2.1), we consider a family of spaces $\mathscr{V}_h$, $h > 0$, approximating $\mathscr{V}$ and based on the finite element method. Then we have the following semidiscrete version of (2.1): given $u_{0,h} \in \mathscr{V}_h$, an approximation of the initial datum $u_0 \in X$, we want to find $u_h(t) \in \mathscr{V}_h$, $t > 0$ such that

$$u_h(0) = u_{0,h} \quad \text{and} \quad \left\langle \frac{\mathrm{d}u_h}{\mathrm{d}t}, w_h\right\rangle = a(u_h, w_h), \quad w_h \in \mathscr{V}_h. \tag{2.2}$$

Since the initial value problem (1.1) is defined in an infinite domain, the usual spaces of finite elements $\mathscr{V}_h$ are not finite dimensional. Let us suppose that $\{\rho_j\}_{j=1}^{\infty}$ are the shape functions defining $\mathscr{V}_h$ in such a way that we have $u_h(t) = \sum_{j=1}^{\infty} u^j(t)\rho_j$ for $t \geqslant 0$. We consider a finite subdomain $[0, x_r]$ such that, for $t \geqslant 0$, if $u_h(t) \in \mathscr{V}_h$ satisfying $\operatorname{supp}(u_h(t)) \subset [0, x_r]$, then $u_h(t) = \sum_{j=1}^{N} u^j(t)\rho_j$, where $N \in \mathbb{N}$ is fixed. In this way, writing $u_{0,h} = \sum_{j=1}^{N} u^j(0)\rho_j$, we obtain the system of ordinary differential equations

$$\begin{aligned} &M\frac{\mathrm{d}}{\mathrm{d}t}\mathbf{u}(t) = A\mathbf{u}(t),\\ &\mathbf{u}(0) = \mathbf{u}_0, \end{aligned} \tag{2.3}$$

where $\mathbf{u}(t) = [u^1(t), \ldots, u^N(t)]^{\mathrm{T}}$, $\mathbf{u_0} = [u_0^1, \ldots, u_0^N]^{\mathrm{T}}$ and the matrices $M$ and $A$ are finite and are given by $M = [M_{ij}] = [\langle \rho_i, \rho_j\rangle]$ and $A = [A_{ij}] = [a(\rho_i, \rho_j)]$, except for the last equations which depend on the boundary conditions that had been used. The choice of this boundary conditions is the subject of the following subsection.

### 2.1. Absorbing boundary conditions for linear finite elements

Since in general the solution of (1.1) is not supported in a finite subdomain of $[0,+\infty)$, in this subsection we construct ABCs at $x = x_r$ when we take linear finite elements as space $\mathscr{V}_h$ for the discretization of Eq. (1.1). We also assume that $\mathrm{supp}(u_0) \subset [0, x_r]$. Let us take a positive parameter $h = x_r/N > 0$, and consider the grid of $[0,+\infty)$ given by $x^j = jh$, $j \geqslant 0$. Let us define

$$\rho_i(x) = \begin{cases} 0 & \text{for } x \notin (x^{i-1}, x^{i+1}), \\ \rho_i^1(x) = \frac{1}{h}(x - x^{i-1}) & \text{for } x \in (x^{i-1}, x^i), \\ \rho_i^2(x) = \frac{1}{h}(x^{i+1} - x) & \text{for } x \in (x^i, x^{i+1}). \end{cases} \tag{2.4}$$

We are interested on the case of a constant potential $V$ in order to obtain ABCs for this space discretization. Then, taking into account that

$$\int_{x^i}^{x^{i+1}} (\rho_i^2(x))^2 \,\mathrm{d}x = \int_{x^i}^{x^{i+1}} (\rho_{i+1}^1(x))^2 \,\mathrm{d}x = \frac{h}{3},$$

$$\int_{x^i}^{x^{i+1}} \rho_i^2(x)\rho_{i+1}^1(x) \,\mathrm{d}x = \frac{h}{6},$$

$$\int_{x^i}^{x^{i+1}} \left(\frac{\mathrm{d}}{\mathrm{d}x}\rho_i^2(x)\right)^2 \mathrm{d}x = \int_{x^i}^{x^{i+1}} \left(\frac{\mathrm{d}}{\mathrm{d}x}\rho_{i+1}^1(x)\right)^2 \mathrm{d}x = \frac{1}{h},$$

$$\int_{x^i}^{x^{i+1}} \frac{\mathrm{d}}{\mathrm{d}x}\rho_i^2(x)\frac{\mathrm{d}}{\mathrm{d}x}\rho_{i+1}^1(x) \,\mathrm{d}x = \frac{-1}{h},$$

we get for $j \geqslant 1$,

$$\frac{1}{6}\left(\frac{\mathrm{d}}{\mathrm{d}t}u^{j-1} + 4\frac{\mathrm{d}}{\mathrm{d}t}u^j + \frac{\mathrm{d}}{\mathrm{d}t}u^{j+1}\right) = \frac{-\mathrm{i}}{ch^2}\left(u^{j-1} - 2u^j + u^{j+1}\right) - \frac{\mathrm{i}V}{6c}\left(u^{j-1} + 4u^j + u^{j+1}\right). \tag{2.5}$$

We denote by $\tilde{u}^j(\lambda)$ the Laplace transform of $u^j(t)$, that is, for $\mathrm{Re}(\lambda) > 0$,

$$\tilde{u}^j(\lambda) = \int_0^\infty \exp(-\lambda s)u^j(s) \,\mathrm{d}s.$$

Since we can suppose that $u^j(0) = 0$, $j \geqslant N - 1$,

$$\widetilde{\frac{\mathrm{d}}{\mathrm{d}t}u^j(t)} = \lambda\tilde{u}^j(\lambda) - u^j(0) = \lambda\tilde{u}^j(\lambda),$$

and from the previous discretization we obtain

$$(6+s)\tilde{u}^{j-1}(\lambda) + (-12+4s)\tilde{u}^j(\lambda) + (6+s)\tilde{u}^{j+1}(\lambda) = 0, \tag{2.6}$$

where

$$s = h^2(V - \mathrm{i}c\lambda). \tag{2.7}$$

**Theorem 2.1.** *The TBC for the right boundary $x = x_r$ is given by*

$$\tilde{u}^{N-1}(\lambda) = r_-(s)\tilde{u}^N(\lambda), \tag{2.8}$$

*where*

$$r_-(s) = \frac{-2s + 6 - \mathrm{i}\sqrt{3s(12-s)}}{s+6}.$$

**Proof.** The solution of (2.6) is given by

$$\tilde{u}^j = C_1 r_+(s)^j + C_2 r_-(s)^j,$$

where $C_1$, $C_2$ are constants and

$$r_{\pm}(s) = \frac{-2s + 6 \pm \mathrm{i}\sqrt{3s(12-s)}}{s+6}, \tag{2.9}$$

being $\sqrt{\cdot}$ the squared root with real positive part, are the roots of the characteristic polynomial equation

$$(s+6)r^2 + (-12+4s)r + (s+6) = 0. \tag{2.10}$$

Now, we want to prove that, in this case, $|r_-(s)| > 1$ and $|r_+(s)| < 1$. We denote $s = x + \mathrm{i}y$, where $x = \mathrm{Re}(s)$ and from (2.7) we deduce that $y = \mathrm{Im}(s) > 0$.

We first prove that the roots (2.9) have modulus 1 only and only if $s \in \mathbb{R}$ and $0 \leqslant s \leqslant 12$. If $s = 12$, it is obvious that the unique root of (2.10) is $r = -1$. On the other hand, if $s \neq 12$, we consider the change of variable

$$r = \frac{1-\rho}{1+\rho}, \tag{2.11}$$

which transforms (2.10) into the new polynomial equation

$$(12-s)\rho^2 + 3s = 0, \tag{2.12}$$

which roots are easily calculated with the formula $\rho = \pm\sqrt{-3s/(12-s)}$. Since the transformation (2.11) applies the right semiplane $\mathrm{Re}(\rho) > 0$ (respectively $\mathrm{Re}(\rho) < 0$) into the interior (respectively exterior) of the unit circle $|r| < 1$, Eq. (2.10) have roots of modulus 1 when (2.12) has purely imaginary roots. This happens when $-3s/(12-s)$ is a negative real number, or equivalently, when $y = 0$ and $x \in [0, 12)$.

On the other hand, the expression (2.9) define continuous (and holomorphic) functions when the variable $s$ is such that $3s(12-s)$ is not a real negative number, that is when $y = 0$ and $x \notin [0, 12]$. Therefore, (2.9) are continuous functions of $s$ when $\mathrm{Im}(s) > 0$.

Finally, it is easily proved that $|r_-(s)| > 1$ for a particular value of $s$ such that $\mathrm{Im}(s) > 0$. From the continuity for $\mathrm{Im}(s) > 0$, we deduce that $|r_-(s)| > 1$ for any $s$ such that $\mathrm{Im}(s) > 0$. In a similar way, $|r_+(s)| < 1$ for any $s$ such that $\mathrm{Im}(s) > 0$.

Since we are considering the right exterior domain $j \geqslant N-1$ it should be $\tilde{u}^j = C_1 r_+^j$. In particular, $\tilde{u}^{N-1} = C_1 r_+^{N-1} = r_+^{-1}\tilde{u}^N = r_-\tilde{u}^N$. □

We are going to construct local ABCs from (2.8). With this aim, we consider an approximation to $r_-(s)$ by a rational function $q(s)$ of exact degree $(2,1)$ that interpolates it at certain nodes $s_1$, $s_2$, $s_3$, $s_4$,

$$r_-(s) \approx q(s) = \frac{\gamma_0 + \gamma_1 s + \gamma_2 s^2}{1 + \gamma_3 s}. \tag{2.13}$$

If we now replace this approximation in the TBC (2.8), and we take into account (2.7), we obtain

$$(1 + h^2\gamma_3(V - \mathrm{i}c\lambda))\tilde{u}^{N-1} = (\gamma_0 + h^2\gamma_1(V - \mathrm{i}c\lambda) + h^4\gamma_2(V - \mathrm{i}c\lambda)^2)\tilde{u}^N.$$

Finally, taking inverse Laplace transform, we get the ABCs

$$\delta_0 u^{N-1} + \delta_1 \frac{\mathrm{d}}{\mathrm{d}t} u^{N-1} = \delta_2 u^N + \delta_3 v^N + \delta_4 \frac{\mathrm{d}}{\mathrm{d}t} v^N, \tag{2.14}$$

where we have introduced the new variable $v^N$ such that

$$\frac{\mathrm{d}}{\mathrm{d}t} u^N = v^N, \tag{2.15}$$

and

$$\delta_0 = 1 + h^2\gamma_3 V, \quad \delta_1 = -\mathrm{i}ch^2\gamma_3, \quad \delta_2 = \gamma_0 + h^2\gamma_1 V + h^4\gamma_2 V^2, \quad \delta_3 = -\mathrm{i}ch^2(\gamma_1 + 2h^2\gamma_2 V), \quad \delta_4 = -h^4\gamma_2 c^2.$$

In order to determine suitable nodes of interpolation, let us take an initial condition $u_0(x) \in L^2(0, x_r)$, and consider its Fourier series

$$u_0(x) = \sum_{k=-\infty}^{\infty} a_k \exp(2\pi \mathrm{i} k x / x_r).$$

Then, we have

$$u_0(x^j) = \sum_{k=-\infty}^{\infty} a_k \mathrm{e}^{\mathrm{i}\tau_k h j},$$

with $\tau_k = 2\pi k / x_r$, and the solution of the semidiscrete problem (2.5) can be written as

$$u^j(t) = \sum_{k=-\infty}^{\infty} a_k \mathrm{e}^{\mathrm{i}\tau_k h j} \mathrm{e}^{-\mathrm{i}\omega(\tau_k h)t},$$

where each term in the series is a plane wave like

$$w^j(t) = a^* \exp(\mathrm{i}\eta^* j - \mathrm{i}\omega(\eta^*)t), \tag{2.16}$$

with $a^* \in \mathbb{C}$ and $\eta^* \in \mathbb{R}$. In order that this plane wave is a solution of (2.5), $\omega(\eta)$ should be determined by the dispersion relation

$$\omega(\eta^*) = \frac{1}{c}\left(V - \frac{6(1-\cos\eta^*)}{h^2(2+\cos\eta^*)}\right).$$

Taking Laplace transform in (2.16), we have

$$\tilde{w}^j(\lambda) = a^* \frac{\exp(\mathrm{i}\eta^* j)}{\lambda + \mathrm{i}\omega(\eta^*)}.$$

Therefore, due to the singularity of this expression, a suitable (real) node to absorb this plane wave is

$$s^* = h^2(V - c\omega(\eta^*)) = \frac{6(1-\cos\eta^*)}{2+\cos\eta^*} \in [0, 12].$$

This reasoning suggests to make the change of variable $s = 6(1-\cos\eta)/(2+\cos\eta)$ in (2.13), getting

$$r_-(\eta) \approx q(\eta) = \frac{\gamma_0 + \gamma_1 \frac{6(1-\cos\eta)}{2+\cos\eta} + \gamma_2 \left(\frac{6(1-\cos\eta)}{2+\cos\eta}\right)^2}{1 + \gamma_3 \frac{6(1-\cos\eta)}{2+\cos\eta}}, \tag{2.17}$$

where $r_-(\eta) = \cos\eta - \mathrm{i}\sin\eta$ if $\sin\eta \geqslant 0$ $(\eta \in [0,\pi])$ and $r_-(\eta) = \cos\eta + \mathrm{i}\sin\eta$ if $\sin\eta < 0$ $(\eta \in [-\pi, 0))$. The approximation (2.17) should be exact at four nodes $\eta = \eta_1, \eta_2, \eta_3, \eta_4$. A suitable node to absorb (2.16) would be $\eta^*$. Finally, the new change of variable $t = \tan(\eta/2)$ gives rise to

$$r_-(\eta) = \frac{1-\mathrm{i}t}{1+\mathrm{i}t} \approx q(\eta) = f(t^2) \quad \text{if } \sin\eta \geqslant 0 \Longleftrightarrow t \geqslant 0, \tag{2.18}$$

$$r_-(\eta) = \frac{1+\mathrm{i}t}{1-\mathrm{i}t} \approx q(\eta) = f(t^2) \quad \text{if } \sin\eta < 0 \Longleftrightarrow t < 0, \tag{2.19}$$

where

$$f(t^2) = \frac{a_0 + a_1 \frac{t^2}{3+t^2} + a_2 \frac{t^4}{(3+t^2)^2}}{1 + a_3 \frac{t^2}{3+t^2}},$$

with $a_0 = \gamma_0$, $a_1 = 12\gamma_1$, $a_2 = 12^2\gamma_2$, $a_3 = 12\gamma_3$. We impose that the approximation ((2.18) and (2.19)) is equal at four nodes $t_1, t_2, t_3, t_4$. If $t_j < 0$, (2.19) should be exact for $t = t_j$, that is to say that (2.18) should we exact for $t = -t_j = |t_j|$. Then, we can conclude that (2.18) should be exact for $t = |t_i|$, $i = 1, \ldots, 4$. On the other hand, now, a suitable node to absorb (2.16) would be $t^* = \tan(\eta^*/2)$.

The choice of the four nodes (which will determine the coefficients of the ABCs) is done in an adaptive way, using Prony's method [19], similarly to [3]. That is, the coefficients of the ABCs will change in each time step in order to absorb the numerical solution that is arriving to the boundary at that time. The idea is that for $x^j$ near the right boundary we approximate

$$u^j(t) \approx \sum_{k=1}^{4} \alpha_k e^{i\tau_k h j} e^{-i\omega(\tau_k h)t}.$$

Once the nodes $t_1$, $t_2$, $t_3$, $t_4$ haven been chosen, the coefficients $a_j$, and therefore those for the ABCs (2.14), are given by

$$\begin{aligned}
a_0 &= (3f_3^2 + 2f_4(9 + 6if_1 - 3f_2 + f_4) - 3f_3(3f_1 + i(-3 + f_2 + f_4)))/\text{den},\\
a_1 &= (27f_1^2 + 18f_2^2 + 45if_3 + 9f_3^2 - 3if_1(9 + 9f_2 - 12if_3 - 7f_4) + 36f_4 - 3if_3f_4\\
&\quad + 4f_4^2 + f_2(-3if_3 - 18(3 + f_4)))/(-\text{den}),\\
a_2 &= (2(81 + 27f_1^2 + 9f_2^2 - 18f_1f_3 + 3f_3^2 + 18f_4 + f_4^2 - 6f_2(9 + f_4)))/\text{den},\\
a_3 &= 3(9f_1^2 + f_3(-if_2 + f_3 + i(-3 + f_4)) + if_1(-9 + 9f_2 + 6if_3 - 5f_4))/(-\text{den}),
\end{aligned}$$

where $\text{den} = 3(f_3^2 + f_3(-3f_1 - i(-3 + f_2 - f_4)) - 2if_1f_4)$ and

$$\begin{aligned}
f_1 &= t_1^* + t_2^* + t_3^* + t_4^*,\\
f_2 &= t_1^*t_2^* + t_1^*t_3^* + t_2^*t_3^* + t_1^*t_4^* + t_2^*t_4^* + t_3^*t_4^*,\\
f_3 &= t_1^*t_2^*t_3^* + t_1^*t_2^*t_4^* + t_1^*t_3^*t_4^* + t_2^*t_3^*t_4^*,\\
f_4 &= t_1^*t_2^*t_3^*t_4^*,
\end{aligned}$$

where $t_j^* = |t_j|$ for $j = 1, \ldots, 4$.

As it will be shown in Section 4, with the use of ABCs given by (2.14) we obtain a good absorption of the solution at the right boundary, similar to the one observed in [1,2] for second order finite differences.

### 2.2. Space discretization: cubic finite elements

Our next purpose is to consider a better spatial discretization in the interior domain while preserving the good absorption at the boundary that we have obtained with the ABCs (2.14) for linear finite elements.

With this purpose, we are going to consider cubic finite elements for the spatial discretization of the interior domain. Moreover, in order to use the ABCs (2.14) we will have to consider linear finite elements near the right boundary and fit them with the cubic finite elements for the interior domain.

Let us define

$$\begin{aligned}
&\sigma_1(x) = (x+1)^2(-2x+1), \quad \tilde{\sigma}_1(x) = x(x+1)^2,\\
&\sigma_2(x) = (x-1)^2(2x+1), \quad \tilde{\sigma}_2(x) = x(x-1)^2,\\
&\sigma^j(x) = \begin{cases} 0 & \text{for } x \notin (x^{j-1}, x^{j+1}),\\ \sigma_1^j(x) = \sigma_1(\frac{x-x^j}{h}) & \text{for } x \in (x^{j-1}, x^j),\\ \sigma_2^j(x) = \sigma_2(\frac{x-x^j}{h}) & \text{for } x \in (x^j, x^{j+1}),\end{cases}\\
&\tilde{\sigma}^j(x) = \begin{cases} 0 & \text{for } x \notin (x^{j-1}, x^{j+1}),\\ \tilde{\sigma}_1^j = h\tilde{\sigma}_1(\frac{x-x^j}{h}) & \text{for } x \in (x^{j-1}, x^j),\\ \tilde{\sigma}_2^j = h\tilde{\sigma}_2(\frac{x-x^j}{h}) & \text{for } x \in (x^j, x^{j+1}),\end{cases}
\end{aligned}$$

and $\rho^j$ as in (2.4). Notice that $\sigma^j$, $\tilde{\sigma}^j$ are the shape functions for the cubic finite elements and $\rho^j$ for the linear finite elements. Since we need to fit the cubic finite elements with the linear ones, we define the functions

$$\begin{aligned}
&\tau^J(x) = \begin{cases} 0 & \text{for } x \notin (x^{J-1}, x^{J+1}),\\ \sigma_1^J(x) & \text{for } x \in (x^{J-1}, x^J),\\ \rho_2^J(x) & \text{for } x \in (x^J, x^{J+1}),\end{cases}\\
&\tilde{\tau}^J(x) = \begin{cases} 0 & \text{for } x \notin (x^{J-1}, x^J),\\ \tilde{\sigma}_1^J(x) & \text{for } x \in (x^{J-1}, x^J),\end{cases}
\end{aligned}$$

where $1 < J < N$ is fixed. In this way, we will consider the set of shape functions

$$\{\tilde{\sigma}^0, \sigma^1, \tilde{\sigma}^1, \sigma^2, \tilde{\sigma}^2, \ldots, \sigma^{J-1}, \tilde{\sigma}^{J-1}, \tau^J, \tilde{\tau}^J, \rho^{J+1}, \ldots, \rho^N\}.$$

Then, the spatial semidiscrete approximation to the solution of (1.1) is

$$u_h(x,t) = \sum_{j=1}^{J-1} u^j(t)\sigma^j(x) + \sum_{j=0}^{J-1} \tilde{u}^j(t)\tilde{\sigma}^j(x) + u^J(t)\tau^J(x) + \tilde{u}^J(t)\tilde{\tau}^J(x) + \sum_{j=J+1}^{N} u^j(t)\rho^j(x),$$

and will have to satisfy the equations

$$\begin{aligned}
&\left\langle \frac{du_h}{dt}, \sigma^j \right\rangle = a(u_h, \sigma^j), \quad j = 1, \ldots, J-1,\\
&\left\langle \frac{\mathrm{d}u_h}{\mathrm{d}t}, \tilde{\sigma}^j \right\rangle = a(u_h, \tilde{\sigma}^j), \quad j = 0, \ldots, J-1,\\
&\left\langle \frac{\mathrm{d}u_h}{\mathrm{d}t}, \tau^J \right\rangle = a(u_h, \tau^J),\\
&\left\langle \frac{\mathrm{d}u_h}{\mathrm{d}t}, \tilde{\tau}^J \right\rangle = a(u_h, \tilde{\tau}^J),\\
&\left\langle \frac{\mathrm{d}u_h}{\mathrm{d}t}, \rho^j \right\rangle = a(u_h, \rho^j), \quad j = J+1, \ldots, N-1.
\end{aligned} \tag{2.20}$$

These equations along with (2.15) and (2.14) give rise to a system of ordinary differential equations like (2.3) with

$$\mathbf{u} = [\tilde{u}^0, u^1, \tilde{u}^1, u^2, \ldots, u^J, \tilde{u}^J, u^{J+1}, \ldots, u^N, v^N].$$

Notice that in Eq. (2.20) we have to compute some integrals whose integrand is the product of the potential $V(x)$ and two shape functions. When the potential is not constant we have used for the numerical experiments of Section 4 a five point Gaussian quadrature formula to approximate those integrals.

Usually, the node $x^J$ will be very near to the right boundary, so that the discretization in the interior domain is basically done with cubic finite elements. Moreover, in practice we are not going to consider the same spatial step size for the cubic finite elements than for the linear ones. In this way, we will have the nodes $x^j = jh$ for $j = 0, \ldots, J$ with the spatial step size $h = x^J/J$ and $x^{j+J} = x^J + j\tilde{h}$ for $j = 1, \ldots, \tilde{J}$, with step size $\tilde{h} = (x_r - x^J)/\tilde{J}$. In practice we will take $\tilde{J}$ quite small ($\tilde{J} = 30$ for instance) and $\tilde{h}$ smaller than $h$.

## 3. Time discretization: symplectic method

The choice of the time discretization is essential in order to obtain good numerical results. We have previously carried out the space discretization, obtaining in this way a system of ordinary differential equations which can be integrated in time with any known time integrator.

An important issue related with this time discretization is the reformulation of the differential equation in (1.1) as a classical Hamiltonian system [15,16,23]. In this way, it is possible to use numerical time integrators originally devised for classical mechanics [21,22]. For this, the differential equation in (1.1) is rewritten as

$$\mathrm{i}\frac{\partial}{\partial t}u(t) = \widehat{H}u(t), \tag{3.1}$$

where the Hamiltonian operator is $\widehat{H} = \frac{1}{c}\left(\frac{\partial^2}{\partial x^2} + V(x)\right)$.

After the space discretization with suitable boundary conditions, for example periodic or vanishing Dirichlet boundary conditions we obtain the $N$-state matrix representation of (3.1),

$$\mathrm{i}\frac{\mathrm{d}\mathbf{c}(t)}{\mathrm{d}t} = \mathbf{H}\mathbf{c}(t), \tag{3.2}$$

where $\mathbf{c}(t) \in \mathbb{C}^{\mathbb{N}}$ is a column vector and $\mathbf{H}$ is in many cases a $N \times N$ real symmetric matrix. Now, introducing the two components $\mathbf{p}(t) = \mathrm{Im}\,\mathbf{c}(t)$, $\mathbf{q}(t) = \mathrm{Re}\,\mathbf{c}(t)$, the Eq. (3.2) is equivalent to the classical Hamiltonian equations of motion

$$\frac{\mathrm{d}\mathbf{p}}{\mathrm{d}t} = -\frac{\partial H}{\partial \mathbf{q}} := \mathbf{f}(\mathbf{p},\mathbf{q}), \quad \frac{\mathrm{d}\mathbf{q}}{\mathrm{d}t} = +\frac{\partial H}{\partial \mathbf{p}} := \mathbf{g}(\mathbf{p},\mathbf{q}), \tag{3.3}$$

with the real Hamiltonian function $H(\mathbf{p},\mathbf{q}) = \frac{1}{2}(\mathbf{q}^{\mathrm{T}} - \mathrm{i}\mathbf{p}^{\mathrm{T}})\mathbf{H}(\mathbf{q} + \mathrm{i}\mathbf{p})$.

From this formulation, it is particularly interesting the use of symplectic integrators [12,15,16,22,23], which are usually implicit. However, the Hamiltonian $H$ is separable, i.e. $H$ is of the form $H(\mathbf{p},\mathbf{q}) = H_1(\mathbf{p}) + H_2(\mathbf{q})$, or, equivalently, the system (3.3) can be written in separable form

$$\frac{\mathrm{d}\mathbf{p}}{\mathrm{d}t} = \mathbf{f}(\mathbf{q}), \quad \frac{\mathrm{d}\mathbf{q}}{\mathrm{d}t} = \mathbf{g}(\mathbf{p}). \tag{3.4}$$

Therefore, it is possible to consider the use of symplectic partitioned Runge–Kutta methods with an important advantage: the computation can be carried out in an explicit form.

However, when we use our ABCs, all the previous considerations are slightly lost. For example, the system of ordinary differential Eq. (2.3) to be solved is not Hamiltonian because the solutions are absorbed at the right boundary and the energy cannot be conserved. Moreover, this system is not separable and the explicitness of the partitioned Runge–Kutta methods is lost.

Another trouble with the use of an explicit partitioned Runge–Kutta method is its stability region. As an example, we consider the fourth order method studied in [23] and specified by the real arrays of coefficients $(b_1, b_2, b_3, b_4, b_5)[B_1, B_2, B_3, B_4]$.

Suppose that we use this method to integrate the scalar test equation $\mathrm{d}y/\mathrm{d}t = \lambda y$, $\lambda \in \mathbb{C}$. Since the eigenvalues of the Schrödinger equation are purely imaginary, we are mainly interested in the case $\lambda = \mathrm{i}\mu$, with $\mu \in \mathbb{R}$.

For this, we use the notation $y = q + \mathrm{i}p$, where $q = \mathrm{Re}(y)$, $p = \mathrm{Im}(y)$ and we obtain the equivalent separable system $\mathrm{d}q/\mathrm{d}t = -\mu p$, $\mathrm{d}p/\mathrm{d}t = \mu q$. For a given step size $k > 0$, the numerical solution $[q_n, p_n]^{\mathrm{T}} \approx [q(nk), p(nk)]^{\mathrm{T}}$ is given by $[q_n, p_n]^{\mathrm{T}} = R^n(k\mu)[q_0, p_0]^{\mathrm{T}}$, where $R(z)$ is the stability matrix of the partitioned Runge–Kutta method. Then we consider the stability interval $\mathscr{I}$ of this method, defined as $\mathscr{I} = \{z \in \mathbb{R} : \rho(\mathbb{R}(\mathbb{z})) \leqslant \mathbb{1}\}$, where $\rho(R(z))$ is the spectral radio of $R(z)$. We have checked numerically that $\mathscr{I}$ is approximately the finite interval $|z| \leqslant 1.88$. This stability interval is not suitable for our problem because the systems of ordinary differential equations obtained after the space discretization are very stiff, i.e. the eigenvalues are very large, corresponding to the arbitrarily large purely imaginary eigenvalues associated to the operator $\frac{-\mathrm{i}}{c}\left(\frac{\partial^2}{\partial x^2} + V(x)\right)$.

Moreover, due to the use of ABCs, the eigenvalues of the ordinary differential system are not purely imaginary. Therefore, it is convenient to consider the stability region $\mathscr{S}$ of this method, defined as $\mathscr{S} = \{z \in \mathbb{C} : \rho(\mathbb{R}(\mathbb{z})) \leqslant \mathbb{1}\}$. However, we have also checked that $\mathscr{S} = \mathscr{I}$ for the previous partitioned Runge–Kutta method, and therefore these ABCs may produce numerical instabilities if we use this time integrator.

Then, we have considered in the present paper the use of the fourth order implicit symplectic Runge–Kutta method studied in [12,21]. As it is mentioned in [12], all the semiplane $\mathrm{Re}(z) \leqslant 0$, except a small island almost circular, is contained in the stability region of this method, which is now defined as $\widetilde{\mathscr{S}} = \{z \in \mathbb{C} :| \mathbb{r}(\mathbb{z}) | \leqslant \mathbb{1}\}$, where $r(z)$ is the stability function of the method. This property is very convenient for our problem.

## 4. Numerical experiments

For the numerical experiments of this paper we are going to consider the equation

$$\mathrm{i}\partial_t u(x,t) = \frac{-1}{2\mu}\partial_{xx} u(x,t) + V(x)u(x,t), \quad x \in [0, x_r], \tag{4.1}$$

where $V(x)$ is a Morse potential $V(x) = D(1 - \exp(-\alpha(x-3)))^2$ (notice that this notation is slightly different from that used in (1.1)). As in [15,16] the parameters are taken to be consistent with an HF molecule, $\mu = 1744.95008$ a.u., $D = 0.225084521$ a.u. and $\alpha = 1.1741$ a.u. Notice that $V(x)$ has a minimum at $x = 3$

and $V(x) \to D$ as $x \to \infty$. For the right boundary $x = x_r$ we will consider the ABCs given by (2.14). In the left boundary $x = 0$, for our purposes it is enough to use a vanishing Dirichlet boundary condition. This choice does not cause reflections to the interior domain because we are going to consider initial conditions that give rise to solutions of the equation travelling to the right, or because the Morse potential $V(x)$ will not allow the solution to arrive to $x = 0$.

First, let us see now the behaviour of ABCs (2.14) with some examples. For the following experiments we will consider Eq. (4.1) with constant potential $V = D$ and with initial condition

$$u_0(x) = \sum_{k=1}^{nw} u_{0k}(x - L_k), \tag{4.2}$$

where each addend $u_{0k}$ is given by the function with Gaussian profile

$$u_{0k}(x) = \exp(\mathrm{i}\eta_k x)\exp(-\gamma x^2) \tag{4.3}$$

evaluated in $x - L_k$, that is, displaced to the right $L_k$ units ($L_k \geqslant 0$), and where $\gamma = \sqrt{D\mu\alpha^2/2}$ (as in [15,16]) and $\eta_j = \mu\tan(\beta_j)$. Therefore, the exact solution for Eq. (4.1) with initial condition (4.2) is

$$u(x,t) = \sum_{k=1}^{nw} u_k(x - L_k, t),$$

where

$$u_k(x,t) = \frac{1}{\sqrt{1 - \frac{4\mathrm{i}t\gamma}{c}}} \exp\left(\frac{-(x + 2\eta_k t/c)^2}{\frac{1}{\gamma} - \frac{4\mathrm{i}t}{c}} + \mathrm{i}\eta_k\left(x + \frac{\eta_k t}{c}\right) + \frac{\mathrm{i}2\mu V t}{c}\right) \tag{4.4}$$

is the exact solution with initial condition (4.3) and $c = -2\mu$.

For the discretization in space studied in Section 2.2, we also need the derivative of the initial condition,

$$\frac{\mathrm{d}}{\mathrm{d}x}u_0(x) = \sum_{k=1}^{nw} \exp\left(\mathrm{i}\eta_k(x - L_k) - \gamma(x - L_k)^2\right)(\mathrm{i}\eta_k - 2\gamma(x - L_k)).$$

In Fig. 1 we have taken $nw = 2$, $x_r = 6$, $\beta_1 = 20°$, $\beta_2 = 15°$, $L_1 = 3$, $L_2 = 4$, so that the solution consists of two waves that arrive to the right boundary almost simultaneously. We have first used (dashed line) linear finite elements for the spatial discretization of the interior domain and the symplectic implicit method of Section 3 for the time integration. We have taken $h = 5.0d - 5$ and a time step $k = 2.5d - 4$. We observe that the solution travels through the interior domain and when it arrives to the right boundary it is absorbed by the effect of the ABCs. We have measured the discrete $L^2$-relative error and we appreciate that although the absorption is very good, the error in the interior domain is too big.

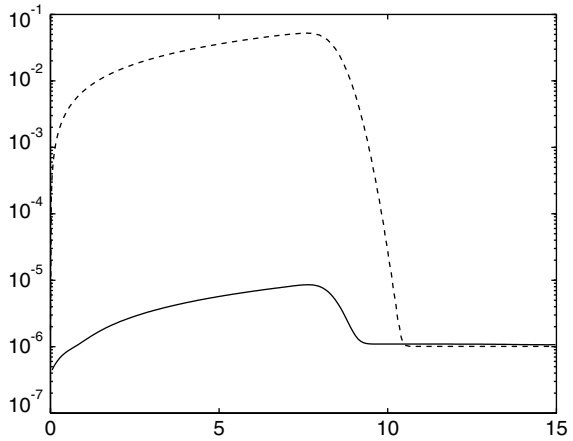


Fig. 1. Local ABCs for linear finite elements. Logarithm of the relative error as a function of time.

Secondly, we have carried out the spatial discretization of the interior domain with cubic finite elements, maintaining the ABCs for linear finite elements at the right boundary. This can be seen in Fig. 1 with continuous line for $h \approx 5.0d - 4$, $\tilde{h} = 1.0d - 5$ (see end of Section 2 for the meaning of $h$ and $\tilde{h}$) and the same discretization in time as for the previous experiment. Observe that the error in the interior domain is much smaller for cubic finite elements even when we have used a bigger value for $h$. On the other hand, the absorption at the right boundary is very similar to the previous experiment.

In Figs. 2 and 3 we see the situation when we consider the initial condition (4.2) with $nw = 1$, $x_r = 6$, $\beta_1 = 20°$ and $L_1 = 3$ and we use cubic finite elements for the discretization in space with $h \approx 5.0d - 4$, $\tilde{h} = 1.0d - 5$ and the same discretization in time as for the previous experiments. More precisely, in Fig. 2 we can see for a fixed time ($t \approx 6$) the error (that is, the modulus of difference between the exact and numerical solution), and the numerical solution. At this moment, the solution has not yet arrived to the boundary. We can observe in Fig. 3 the situation at $t \approx 12$ when the solution should have disappeared from the computational window.

Let us see a numerical experiment for which we have considered Eq. (4.1) with the Morse potential. As initial condition we have taken (4.2) with $nw = 1$, $\beta_1 = -20°$ and $L_1 = 3$. In Fig. 4 we see the modulus of the

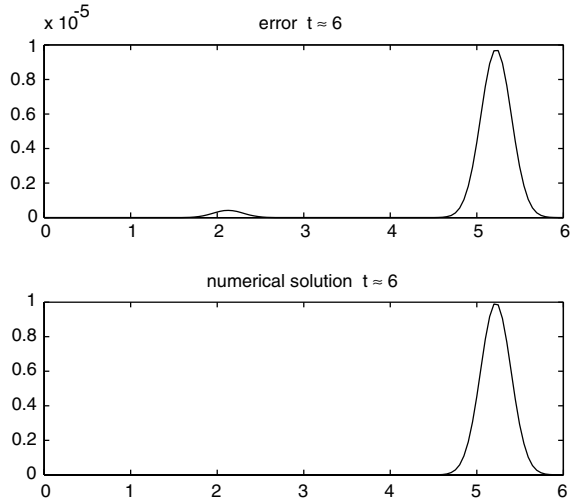


Fig. 2. Error and modulus of the numerical solution for a single Gaussian wave arriving to the right boundary.

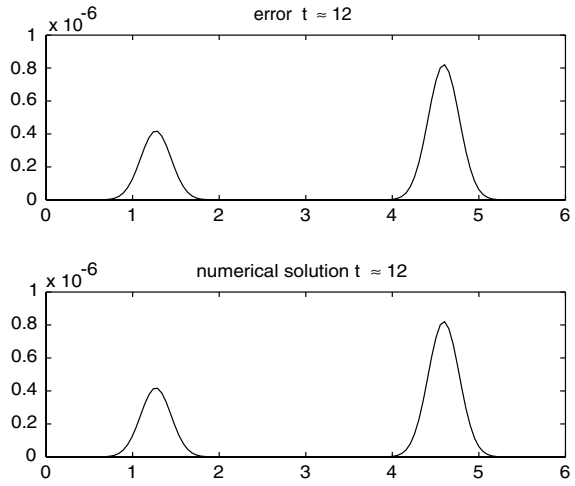


Fig. 3. Error and modulus of the numerical solution for a single Gaussian wave after the absorption at the right boundary.

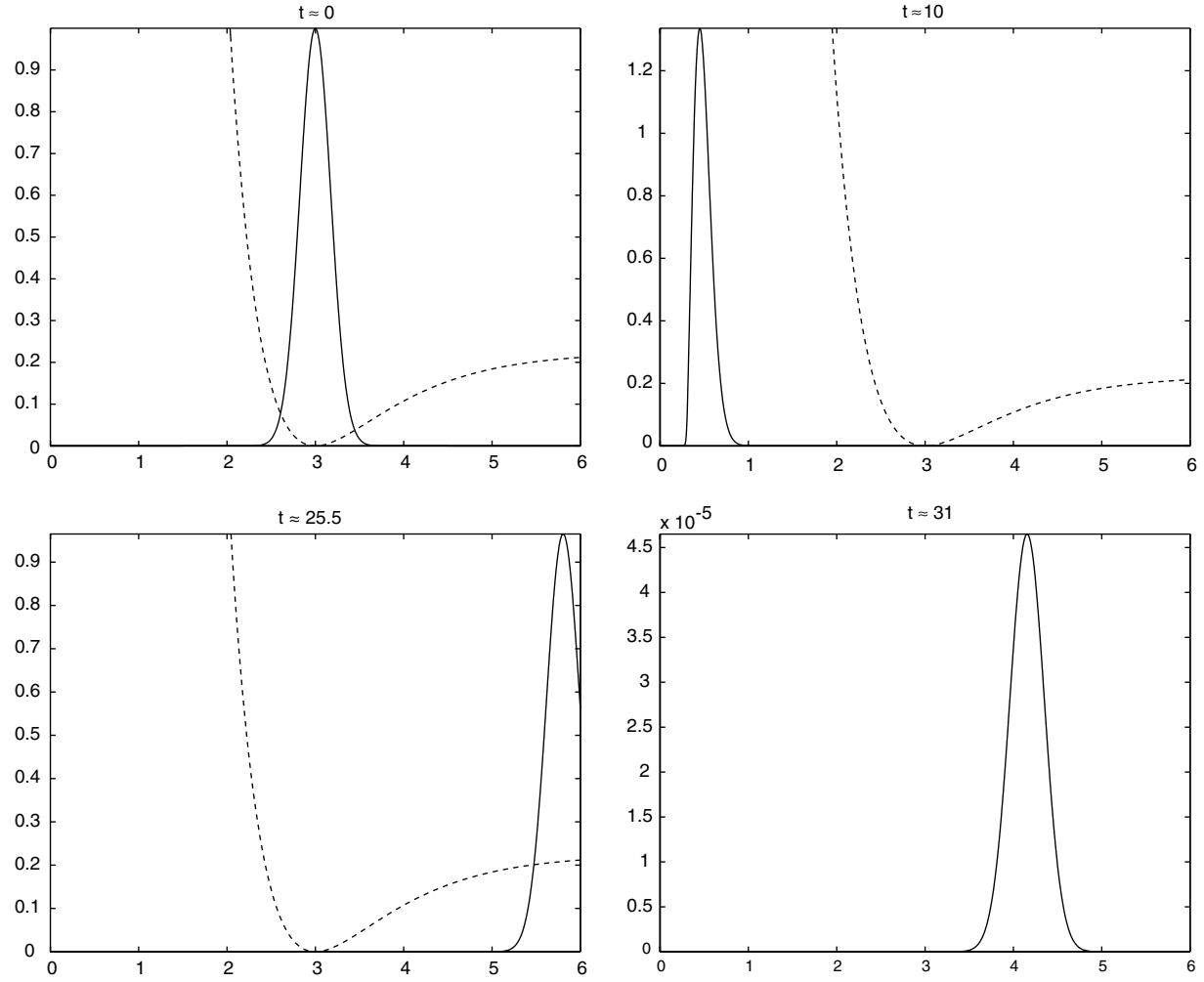


Fig. 4. Modulus of the numerical solution (—) and Morse potential (---).

numerical solution at four different fixed times when we discretize the equation with cubic finite elements along with the ABCs (2.14) in the way we have described in Section 2. In the first three figures we can also see the Morse potential with dashed line. We have considered the interior domain $[0, 6]$, spatial step sizes $h = 5.0d - 4$, $\tilde{h} = 5.0d - 5$ and we have set $\tilde{J} = 30$ so that $x^J$ is very close to $x_r = 6$. The time discretization has been done with the implicit symplectic integrator described in Section 3 with step size $k = 5.0d - 4$. For $t = 0$ we can see the modulus of the initial condition. At $t \approx 10$ the solution has already moved to the left boundary and is starting to move to the right. When $t \approx 25.5$ the solution is a wave arriving to the right boundary and is being absorbed by the ABCs. Finally, at $t \approx 31$ the exact solution would have disappeared from the computational window and what we observe in Fig. 4 for this time is the reflection caused by the ABCs and the error due to the spatial discretization in the interior domain.

## References

[1] I. Alonso-Mallo, N. Reguera, Weak ill-posedness of spatial discretizations of absorbing boundary conditions for Schrödinger-type equations, SIAM J. Numer. Anal. 40 (2002) 134–158.
[2] I. Alonso-Mallo, N. Reguera, Discrete absorbing boundary conditions for Schrödinger-type equations. Construction and error analysis, SIAM J. Numer. Anal. 41 (2003) 1824–1850.
[3] I. Alonso-Mallo, N. Reguera, Discrete absorbing boundary conditions for Schrödinger-type equations. Practical implementation, Math. Comput. 73 (2004) 127–142.

[4] I. Alonso-Mallo, N. Reguera, One dimensional cubic nonlinear Schrödinger equation with local absorbing boundary conditions, submitted for publication.
[5] X. Antoine, C. Besse, Unconditionally stable discretization schemes of non-reflecting boundary conditions for the one-dimensional Schrödinger equation, J. Comput. Phys. 188 (2003) 157–175.
[6] X. Antoine, C. Besse, V. Mouysset, Numerical schemes for the simulation of the two-dimensional Schrödinger equation using non-reflecting boundary conditions, Math. Comput. 73 (2004) 1779–1799.
[7] A. Arnold, M. Ehrhard, Discrete transparent boundary conditions for wide angle parabolic equations in underwater acoustics, J. Comput. Phys. 145 (1998) 611–638.
[8] A. Arnold, M. Ehrhardt, I. Sofronov, Discrete transparent boundary conditions for the Schrödinger equation: fast calculation, approximation, and stability, Commun. Math. Sci. 1 (2003) 501–556.
[9] J.P. Bérenger, A perfectly matched layer for the absorption of electromagnetic waves, J. Comput. Phys. 114 (1994) 185–200.
[10] F. Collino, Perfectly matched absorbing layers for the paraxial equations, J. Comput. Phys. 131 (1997) 164–180.
[11] B. Engquist, A. Majda, Absorbing boundary conditions for the numerical simulation of wave, Math. Comput. 31 (1977) 629–651.
[12] J. de Frutos, J.M. Sanz-Serna, Classical numerical integrators for wave-packet dynamics, J. Comput. Phys. 103 (1992) 160–168.
[13] L. Di Menza, Transparent and absorbing boundary conditions for the Schrödinger equation in a bounded domain, Numer. Funct. Anal. Optim. 18 (1997) 759–775.
[14] T. Fevens, H. Jiang, Absorbing boundary conditions for the Schrödinger equation, SIAM J. Sci. Comput. 21 (1999) 255–282.
[15] S.K. Gray, D.E. Manolopoulos, Symplectic integrators tailored to the time-dependent Schrödinger equation, J. Chem. Phys. 104 (1996) 7099–7112.
[16] S.K. Gray, J.M. Verosky, Classical Hamiltonian structures in wave packet dynamics, J. Chem. Phys. 100 (1994) 5011–5022.
[17] T. Hagstrom, Radiation boundary conditions for the numerical simulation of waves. Acta numerica, 1999Acta Numer., 8, Cambridge University Press, Cambridge, 1999, pp. 47–106.
[18] T. Hagstrom, New results on absorbing layers and radiation boundary conditions, in: Topics in Computational Wave PropagationLecture Notes in Computer Science Engineering, 31, Springer, Berlin, 2003, pp. 1–42.
[19] S.L. Marple Jr., Digital Spectral Analysis with Applications, Prentice Hall, Englewood Cliffs, 1987.
[20] A. Pazy, Semigroups of Linear Operators and Applications to Partial Differential Equations, Springer-Verlag, New York, 1983.
[21] J.M. Sanz-Serna, L. Abia, Order conditions for canonical Runge–Kutta schemes, SIAM J. Numer. Anal. 28 (1991) 1081–1096.
[22] J.M. Sanz-Serna, M.P. Calvo, Numerical Hamiltonian problems, Chapman & Hall, London, 1994.
[23] J.M. Sanz-Serna, A. Portillo, Classical numerical integrators for wave-packet dynamics, J. Chem. Phys. 104 (1996) 2349–2355.
[24] F. Schmidt, P. Deuflhard, Discrete transparent boundary conditions for the numerical solution of Fresnel's equation, Comput. Math. Appl. 29 (1995) 53–76.
[25] F. Schmidt, D. Yevick, Discrete transparent boundary conditions for Schrödinger-type equations, J. Comput. Phys. 134 (1997) 96–107.
[26] S.V. Tsynkov, Numerical solution of problems on unbounded domains. A review, Appl. Numer. Math. 27 (1998) 465–532.